Small deformations of extreme Kerr black hole initial data

2011 Class. Quantum Grav. 28 075003

(http://iopscience.iop.org/0264-9381/28/7/075003)

IOP PUBLISHING CLASSICAL AND QUANTUM GRAVITY

Class. Quantum Grav. **28** (2011) 075003 (20pp) doi:10.1088/0264-9381/28/7/075003

Small deformations of extreme Kerr black hole initial data

Sergio Dain[1,2] **and María E Gabach Clément**[1]

[1] Facultad de Matemática, Astronomía y Física, FaMAF, Universidad Nacional de Córdoba, Instituto de Física Enrique Gaviola, IFEG, CONICET, Ciudad Universitaria, (5000) Córdoba, Argentina
[2] Max Planck Institute for Gravitational Physics, Albert Einstein Institute, Am Mühlenberg 1, D-14476 Potsdam, Germany

E-mail: dain@famaf.unc.edu.ar and gabach@famaf.unc.edu.ar

Received 19 August 2010, in final form 28 January 2011
Published 28 February 2011
Online at stacks.iop.org/CQG/28/075003

Abstract
We prove the existence of a family of initial data for Einstein equations which represent small deformations of the extreme Kerr black hole initial data. The data in this family have the same asymptotic geometry as extreme Kerr. In particular, the deformations preserve the angular momentum and the area of the cylindrical end.

PACS numbers: 04.70.−s, 04.20.Jb, 04.20.Dw

1. Introduction

Black holes are one of the most spectacular predictions of general relativity. There is growing experimental evidence that indicates that black holes do indeed exist in nature. Among the most impressive ones is the evidence for the existence of a supermassive black hole in the center of our galaxy (see the review article [37]).

In vacuum, the only stationary black hole is expected to be the Kerr black hole, characterized by the mass m and the angular momentum J (see [13] and references therein for updated results on this problem). The Kerr black hole satisfies the inequality $m \geqslant \sqrt{|J|}$. The limit case $m = \sqrt{|J|}$ is called the extreme black hole. It represents the stationary black hole with maximum amount of angular momentum per mass unit. The extreme limit $\sqrt{|J|} \to m$ is singular because the geometry of the spacetime changes at the limit. This is somehow to be expected since the extreme case is the borderline between a black hole and a spacetime with a naked singularity (i.e. the Kerr solution with $0 < m < \sqrt{|J|}$).

There exist relevant reasons to study extreme black holes. The first one is that there is good experimental evidence for the existence of nearly extreme black holes in the universe (see [35] for experimental evidence of a black hole with $J/m^2 > 0.98$). Then, it is important to understand the dynamics of black holes near the extreme limit. The second reason is less

clear but, we believe, equally important. As it often happens in physical theories, solutions that arise as asymptotic limits are simpler than other solutions and they provide useful insights into the theory. In the set of solutions of Einstein equation, extreme black holes represent a kind of barrier that divides black holes and naked singularities. From the pure classical point of view, there is evidence that extreme black holes have some special properties that make them simpler than non-extreme ones (see the discussion in [21]). Also from a completely different perspective, namely holographic dualities, particular features of extreme black holes play an important role (see [4, 27], see also the review article [3]). It appears that extreme black holes have a deep mathematical structure that is still to be uncovered.

Finally, there is a third reason to study extreme black holes. In the problem of extreme black hole initial conditions (which is the subject of this paper), a particular kind of geometry appears: geometries with cylindrical ends. These geometries have proven to be very useful in numerical computations of black hole collisions; they are called 'trumpet' initial conditions in this context. It is important to emphasize that the presence of a cylindrical end does not imply that the initial data are stationary (in particular, it does not imply that the data are the extreme Kerr black hole initial data). The cylindrical end imposes only asymptotic conditions to the data. Non-stationary cylindrical initial data have been constructed numerically in [24, 28, 32]. In [23, 26] their existence has been proved analytically. Numerical studies (see [28–30]) suggest that binary black holes with cylindrical geometries are simpler to evolve than initial data with multiple asymptotically flat ends (also called 'punctures' in numerical relativity).

As a first step to understand the dynamics near an extreme Kerr black hole, in this paper we study small deformations of the extreme Kerr black hole initial conditions. We prove the existence of a family of initial data that are close to extreme Kerr initial data. In particular, the asymptotic geometry of these initial data is the same as the extreme Kerr geometry. These data are, generically, non-stationary. It is important to emphasize that the existence of these initial conditions is, *a priori*, by no means obvious due to the character of the extreme Kerr geometry.

We would also like to comment on the mathematical techniques used in the proof of our results. The proof of our main theorem essentially deals with existence and uniqueness of solutions of the Lichnerowicz equation. This equation has been extensively studied in the literature. See the review article [6] and references therein. In particular, different kinds of boundary and asymptotic fall-off conditions have been analyzed for this equation: closed manifolds [31], asymptotically flat manifolds [11] and asymptotically flat manifold with an inner horizon [17, 34]. However, there are no results concerning cylindrical fall-off conditions. One of the goals of this paper is precisely to initiate the study of this kind of boundary condition. Using adapted coordinates, the fall-off conditions at the cylindrical end translate into singular behavior of the conformal factor at the origin. To deal with it, we have to use non-standard functional spaces with weight both at infinity and at the origin. This is one of the main technical difficulties of this problem.

The paper is organized as follows. We begin in section 2 with a review of some of the main properties of the extreme Kerr black hole. Then we state our main result avoiding technical details. We also discuss how the cylindrical geometry is preserved along the evolution. In section 3 we state our main theorem in a precise form and prove it. We conclude the paper with a discussion of some relevant open problems in section 4. Finally, we have included three appendices. In appendix A we prove a decay property of the Sobolev spaces used in our proof. In appendix B we prove a property of the extreme Kerr initial data which plays a central role in the proof. Appendix C is a brief summary of the implicit function theorem, which is the central analytical tool used in the proof.

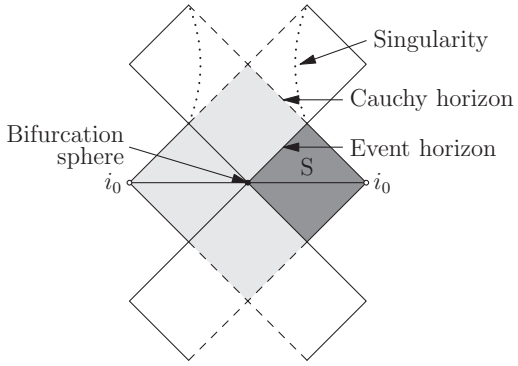

Figure 1. Conformal diagram of the Kerr black hole in the non-extreme case.

2. Main result

Consider the Kerr black hole with mass m and angular momentum J. In the non-extreme case (i.e. $m > \sqrt{|J|}$) the maximal analytical extension of the metric has the well-known global structure shown in figure 1 (see [7, 8] and also [9]). Take the spacelike surface S drawn in this figure. This surface runs from one spacelike infinity (denoted by i_0) to the other. The topology of this surface is $S = \mathbb{S}^2 \times \mathbb{R}$. The triple (S, h_{ij}, K_{ij}), where h_{ij} is the induced intrinsic metric on S and K_{ij} is the second fundamental form of S, constitute an initial dataset for Einstein equations. That is, they are solutions of the constraint equations

$$D_j K^{ij} - D^i K = 0, \tag{1}$$

$$R - K_{ij} K^{ij} + K^2 = 0, \tag{2}$$

where D and R are the Levi-Civita connection and the Ricci scalar associated with h_{ij}, and $K = K_{ij} h^{ij}$. In these equations the indices are moved with the metric h_{ij} and its inverse h^{ij}.

The Riemannian manifold (S, h_{ij}) has two asymptotically flat ends (see figure 2). This asymptotic geometry is identical to the analogous slice of Kruskal extension for the Schwarzschild black hole. The surface S in figure 1 corresponds to a slice $t = 0$ of the Boyer–Lindquist coordinates $(t, \tilde{r}, \theta, \phi)$ in Kerr metric (see appendix B). It intersects the bifurcation sphere (denoted by a dark dot in figure 1 and by a dark circle in figure 2). The slice is isometric across this sphere. The bifurcation sphere on the slice is both a minimal surface and an apparent horizon. In these coordinates, spacelike infinity i_0 is represented by the limit $\tilde{r} \to \infty$. The intrinsic metric and the second fundamental form satisfy the standard asymptotically flat fall-off conditions

$$h_{ij} = \delta_{ij} + o(\tilde{r}^{-1/2}), \qquad \partial h_{ij} = o(\tilde{r}^{-3/2}), \tag{3}$$

$$K_{ij} = O(\tilde{r}^{-3}), \tag{4}$$

as $r \to \infty$, where δ_{ij} is the flat metric. The strong fall-off behavior of the second fundamental form implies that the linear momentum of the initial data vanishes. The angular momentum is contained in the term $O(\tilde{r}^{-3})$ of K_{ij}.

The maximal development of the initial dataset (S, h_{ij}, K_{ij}) is shown in light gray in figure 1. This region does not cover the whole analytical extension (as in the case of Schwarzschild's) and it has a smooth boundary in the spacetime. This boundary is known

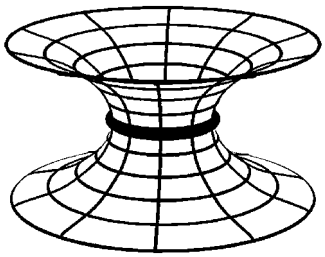

Figure 2. Embedding diagram of a two-dimensional slice ($t = \text{const.}$, $\theta = \pi/2$) of the extended non-extreme Kerr solution. The dark circle in the middle represents the minimal surface (throat) connecting two asymptotically flat ends.

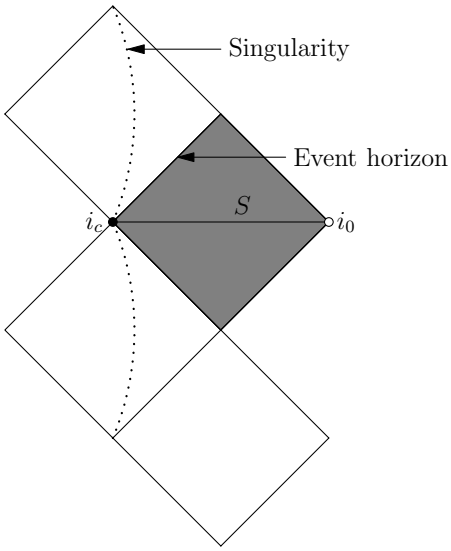

Figure 3. Conformal diagram for the extreme Kerr black hole. The cylindrical end is denoted by i_c.

as the Cauchy horizon. In dark gray the domain of outer communications is shown, which is bounded by the black hole event horizon.

In the extreme case $m = \sqrt{|J|}$, the global structure of the spacetime changes. The maximal analytical extension is shown in figure 3. The spacelike surface S has the same topology $\mathbb{S}^2 \times \mathbb{R}$ as in the non-extreme case; however, the asymptotic geometry of the Riemannian manifold (S, h_{ij}) is different. It has one asymptotically flat end and one cylindrical end, see figure 4. The cylindrical end asymptotically approaches the event horizon. Contrary to the asymptotically flat case, this end is in the strong field region of the spacetime. Note that (S, h_{ij}) is a complete Riemannian manifold without boundary which lies completely in the black hole exterior region. Let us take a closer look at the structure of the cylindrical end. In isotropic coordinates (r, θ, ϕ), with $r := \tilde{r} - m$ (see appendix B), the induced metric on S has the form

$$h^0_{ij} = \Phi_0^4 \tilde{h}^0_{ij}, \qquad \tilde{h}^0 = e^{2q_0}(\mathrm{d}r^2 + r^2\,\mathrm{d}\theta^2) + r^2 \sin^2\theta\,\mathrm{d}\phi^2, \tag{5}$$

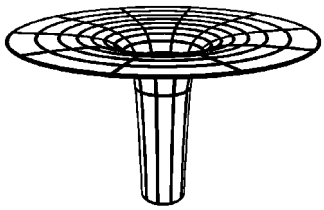

Figure 4. Embedding diagram of a two-dimensional slice ($t = \text{const.}$, $\theta = \pi/2$) of the extreme Kerr solution. There is an asymptotically flat end (top) and an asymptotically cylindrical end (bottom).

where Φ_0 and q_0 are given by equation (B.6) in appendix B. The extrinsic curvature is given by

$$K^0_{ij} = \frac{2}{\eta} S_{(i}\eta_{j)}, \qquad S_i = \frac{1}{\eta}\epsilon_{ijk}\eta^j \partial^k \omega_0, \tag{6}$$

where η^i is the axial Killing vector, η the square of its norm (see equation (B.2)), ϵ_{ijk} denotes the volume element with respect to the metric h_{ij} and ω_0 is given by (B.7). The advantage of this particular form of writing K^0_{ij} is that it is easy to check from (6) that K^0_{ij} satisfies the momentum constraint (1). We will discuss and use this fact in section 3. In particular, we have that K^0_{ij} is trace-free:

$$K^0 = 0. \tag{7}$$

That is, these initial data are maximal surfaces.

In isotropic coordinates, the asymptotically flat end is given by the limit $r \to \infty$ and the cylindrical end by the limit $r \to 0$. The radial coordinate r is a good coordinate in the asymptotically flat end since the metric and the extrinsic curvature take the asymptotic form (3).

On the other hand, in the limit $r \to 0$ the conformal factor Φ_0 blows up. This is, however, just a coordinate problem. To see this, let $s = -\ln r$; then, the cylindrical end corresponds to $s \to \infty$, and the metric has the form

$$h^0 = (\sqrt{r}\Phi_0)^4 (e^{2q_0}(\mathrm{d}s^2 + \mathrm{d}\theta^2) + \sin^2\theta\, \mathrm{d}\phi^2). \tag{8}$$

The functions $\sqrt{r}\Phi_0$ and q_0 are smooth and uniformly bounded in the whole range $-\infty < s < \infty$ (see lemma B.2). In particular, the Riemannian manifold $\left(S, h^0_{ij}\right)$ has bounded curvature.

It is interesting to note (although we will not make use of it) that the metric (8) and the second fundamental form (6) have a well-defined limit $s \to \infty$ as initial data. Namely

$$h^0 = m^2(1+\cos^2\theta)(\mathrm{d}s^2 + \mathrm{d}\theta^2) + \frac{4m^2\sin^2\theta}{(1+\cos^2\theta)}\,\mathrm{d}\phi^2 \qquad \text{as} \quad s \to \infty, \tag{9}$$

where we have used the limits (B.10)–(B.11). The extrinsic curvature K^{ij}_0 has the form (6) where ω_0 is replaced by its limiting value (B.12) and all the other quantities are computed with respect to the metric (9). These are in fact solutions of the constraint equations (1)–(2). They isolate the cylindrical geometry cutting off the asymptotically flat end. In particular, the metric (9) has a non-negative Ricci scalar, given by the limit (B.13) and it has another symmetry, namely translations in s. These limit initial data are slices $t = \text{constant}$ of the four-dimensional vacuum geometry described in [4], known as the the near-horizon extreme Kerr. This geometry has also been studied in [9] (see equation (5.63) in that reference).

A relevant parameter for extreme black hole data is the area of the cylindrical end. Consider the area $A(r)$ of the surfaces $r =$ constant of the metric (5). In the limit $r \to 0$ we have

$$A_0 = \lim_{r\to 0} A(r) = 8\pi m^2. \tag{10}$$

For extreme Kerr, this corresponds to the area of the black hole event horizon. Finally, for completeness, let us mention that the ergoregion on S is given in these coordinates by

$$0 < r < m \sin\theta. \tag{11}$$

We have described a particular class of initial datasets for the extreme Kerr black hole which run from i_c to i_0. There exist similar initial datasets in Reissner–Nordström and Kerr–Newman black holes. Remarkably enough, for a Schwarzschild black hole there also exist initial data that have the same asymptotic geometry (see [29] and references therein). All these examples are stationary. Moreover, all these data arise as a singular limit in which the geometry changes. The first numerical evidence for the existence of non-stationary cylindrical data with a similar structure as the one described above was given in [24] and the first analytical proof was provided in [23, 26]. These data are also obtained as a singular limit from non-extreme data. The point we want to address in this paper is as follows: given extreme Kerr initial data, does there exist a neighborhood of similar data? The following theorem, which constitutes the main result of this paper, gives an affirmative answer to this question.

Theorem 2.1. *Let $\left(S, h^0_{ij}, K^0_{ij}\right)$ be the extreme Kerr dataset described above with angular momentum J and mass $m = \sqrt{|J|}$. Then there is a small $\lambda_0 > 0$ such that for $-\lambda_0 < \lambda < \lambda_0$ there exists a family of initial datasets $(S, h_{ij}(\lambda), K_{ij}(\lambda))$ (i.e. solutions of the constraints on S) with the following properties.*

(i) We have $h_{ij}(0) = h^0_{ij}$ and $K_{ij}(0) = K^0_{ij}$. The family is differentiable in λ and it is close to extreme Kerr with respect to an appropriate norm which involves two derivatives of the metric.

(ii) The data have the same asymptotic geometry as the extreme Kerr initial dataset. The angular momentum and the area of the cylindrical end in the family do not depend on λ; they have the same value as in $\left(S, h^0_{ij}, K^0_{ij}\right)$, namely J and $8\pi|J|$, respectively.

(iii) The data are axially symmetric and maximal (i.e. $K(\lambda) = 0$).

In section 3 we provide a more precise version of this theorem (theorem 3.1). Let us discuss here other relevant properties of the initial data family $(S, h_{ij}(\lambda), K_{ij}(\lambda))$.

We mention that the angular momentum of the family remains constant, the total mass however is not. As a consequence of the general theorems [12, 22] we have the following inequality for all λ:

$$m(\lambda) \geqslant \sqrt{|J|}, \tag{12}$$

with equality only for $\lambda = 0$ (i.e. for extreme Kerr). This family realizes the local minimum behavior of extreme Kerr studied in [18].

Inequality (12) allows us to define the following positive quantity:

$$E(\lambda) = m(\lambda) - \sqrt{|J|}. \tag{13}$$

The energy E provides (if we assume cosmic censorship) an upper bound for the total amount of radiation emitted by the system at null infinity for these initial data (see the discussion in [21]).

Let us consider now some aspects of the evolution of these data. In the asymptotically flat case, it is well known that the asymptotic behavior (3) is preserved by evolution if we impose appropriate fall-off conditions for the lapse and shift. This is of course important, since it is

related to conservation of total mass in the spacetime. The natural question is whether this kind of persistence under evolution also holds for the cylindrical asymptote. To study this question we need non-stationary data as the ones constructed here.

Let us consider a member of the family for some $\lambda \neq 0$ (we will suppress the λ in the notation in the following). Take a short period of time t; then, we have

$$h_{ij}(t) \approx h_{ij}(0) + \dot{h}_{ij}(0)t, \tag{14}$$

$$K_{ij}(t) \approx K_{ij}(0) + \dot{K}_{ij}t, \tag{15}$$

where dot denotes the time derivative. The time derivatives $\dot{h}_{ij}$, $\dot{K}_{ij}$ can be computed using the evolution equations

$$\dot{h}_{ij} = 2\alpha K_{ij} + \mathcal{L}_\beta h_{ij}, \tag{16}$$

$$\dot{K}_{ij} = \nabla_i\nabla_j\alpha + \mathcal{L}_\beta K_{ij} + \alpha\big(2K_i^k K_{jk} - K K_{ij} - R_{ij}\big), \tag{17}$$

where α and β^i are the lapse and shift of the foliation, $\mathcal{L}$ denotes the Lie derivative and R_{ij} is the Ricci tensor of h_{ij}. Lapse and shift can be of course arbitrarily prescribed, independently of the initial conditions. We want to argue that if we chose the lapse and shift with appropriate decay conditions at the cylindrical end, then the cylindrical fall properties are preserved along the whole foliation. This is completely analogous to the asymptotically flat case.

If we want to preserve the cylindrical geometry under the evolution, we must have

$$\lim_{s\to\infty} \dot{h}_{ij} = 0, \qquad \lim_{s\to\infty} \dot{K}_{ij} = 0. \tag{18}$$

From equations (16) to (17) we deduce the conditions for the lapse

$$\lim_{s\to\infty} \alpha = \lim_{s\to\infty} \partial\alpha = \lim_{s\to\infty} \partial^2\alpha = 0, \tag{19}$$

and the shift

$$\lim_{s\to\infty} \beta^i = \lim_{s\to\infty} \partial\beta^i = 0, \tag{20}$$

where ∂ denotes partial derivatives with respect to the space coordinates. Note that for the particular Boyer–Lindquist foliation in extreme Kerr these requirements are satisfied (see equations (B.8)–(B.9) in appendix B). Conditions (19) and (20) are analogous to the asymptotically flat conditions for lapse and shift.

In this paper, we have assumed vacuum for simplicity. We expect that an analogous result as theorem (5) holds for the Kerr–Newman extreme black hole. In that case, inequality (12) should be replaced by it generalized charged version recently proved in [14, 15].

3. Proof of the main result

A particular feature of axial symmetry is that it allows one to reduce the constraint equations (1)–(2) to just one scalar equation for a conformal factor (the so-called Lichnerowicz equation). This procedure is well known (see, for example, [22] and references therein). Let us briefly review it. Consider the metric

$$\tilde{h}_{ij} = e^{-2q}(\mathrm{d}r^2 + r^2\,\mathrm{d}\theta^2) + r^2\sin^2\theta\,\mathrm{d}\varphi^2, \tag{21}$$

where $q = q(r,\theta)$ is an arbitrary function. This metric will be used as a conformal background for the physical metric h_{ij}. We first discuss how to construct solutions of the momentum constraint (1) from an arbitrary axially symmetric potential $\omega(r,\theta)$. Consider the following tensor:

$$\tilde{K}^{ij} = \frac{2}{\rho^2}\tilde{S}^{(i}\eta^{j)}, \tag{22}$$

where

$$\tilde{S}^i = \frac{1}{2\rho^2}\tilde{\epsilon}^{ijk}\eta_j\partial_k\omega, \tag{23}$$

and $\tilde{\epsilon}_{ijk}$ denotes the volume element with respect to $\tilde{h}_{ij}$, $\tilde{D}$ is the connection with respect to $\tilde{h}_{ij}$ and $\rho = r\sin\theta$ is the cylindrical radius. The indices on tilde quantities are moved with $\tilde{h}_{ij}$ and its inverse $\tilde{h}^{ij}$. The tensor $\tilde{K}^{ij}$ is symmetric, trace free and satisfies the following equation (see, for example, the appendix in [16]):

$$\tilde{D}_i\tilde{K}^{ij} = 0 \tag{24}$$

for arbitrary q and ω. Equation (24) essentially solves (up to a conformal factor) the momentum constraint (1). Assume that we have a solution Φ of the Lichnerowicz equation

$$\Delta_{\tilde{h}}\Phi - \frac{\tilde{R}}{8}\Phi = -\frac{\tilde{K}_{ij}\tilde{K}^{ij}}{8\Phi^7}, \tag{25}$$

where $\Delta_{\tilde{h}}$ is the Laplacian with respect to $\tilde{h}_{ij}$ and $\tilde{R}$ is the Ricci scalar of $\tilde{h}_{ij}$. To solve equation (25) we need to impose appropriate boundary conditions. In our case, these conditions are asymptotic flat fall-off conditions at infinity (i.e. in the limit $r \to \infty$) and conditions at the origin $r = 0$ that represent the cylindrical end. Both conditions will be incorporated in the definition of the weighted Sobolev space used in the proof of theorem 3.1, as we will explain below.

Consider the rescaling

$$h_{ij} = \Phi^4\tilde{h}_{ij}, \qquad K_{ij} = \Phi^{-2}\tilde{K}_{ij}. \tag{26}$$

Then, as a consequence of (24) the pair (h_{ij}, K_{ij}) satisfies the constraints (1)–(2). That is, the problem reduces to solving equation (25). This equation can be written in the following remarkably simple form in axial symmetry

$$\Delta\Phi = -\frac{(\partial\omega)^2}{16\rho^4\Phi^7} - \frac{\Delta_2 q}{4}\Phi, \tag{27}$$

where Δ and Δ_2 are flat Laplace operators in three and two dimensions, respectively (see (B.14)). In particular, extreme Kerr initial data satisfy this equation, namely

$$\Delta\Phi_0 = -\frac{(\partial\omega_0)^2}{16\rho^4\Phi_0^7} - \frac{\Delta_2 q_0}{4}\Phi_0. \tag{28}$$

The idea is to perturb equation (27) around the extreme Kerr solution by taking

$$q_0 + \lambda q, \qquad \omega_0 + \lambda\omega \tag{29}$$

for some fixed functions q and ω and small λ, and then to find a solution u defined by

$$\Phi = \Phi_0 + u. \tag{30}$$

Inserting (29) and (30) in equation (27) and using (28) we obtain our final equation

$$G(\lambda, u) = 0, \tag{31}$$

where we have defined

$$G(\lambda, u) = \Delta u + \frac{(\partial w_0 + \lambda\partial w)^2}{16\rho^4(\Phi_0 + u)^7} - \frac{\partial w_0^2}{16\rho^4\Phi_0^7} + \lambda\frac{\Delta_2 q}{4}(\Phi_0 + u) + \frac{\Delta_2 q_0}{4}u. \tag{32}$$

Then, theorem 2.1 is a direct consequence of the following existence theorem for equation (31).

Theorem 3.1. *Let $w \in C_0^\infty(\mathbb{R}^3 \setminus \Gamma)$ and $q \in C_0^\infty(\mathbb{R}^3 \setminus \{0\})$. Then, there is $\lambda_0 > 0$ such that for all $\lambda \in (-\lambda_0, \lambda_0)$ there exists a solution $u(\lambda) \in H'^2_{-1/2}$ of equation (31). The solution $u(\lambda)$ is continuously differentiable in λ and it satisfies $\Phi_0 + u(\lambda) > 0$. Moreover, for small λ and small u (in the norm $H'^2_{-1/2}$) the solution $u(\lambda)$ is the unique solution of equation (31).*

We have used the following notation: Γ denotes the axis $\rho = 0$, $C_0^\infty(\Omega)$ are smooth functions with compact support in Ω and $H'^2_{-1/2}$ denotes the Sobolev weighted spaces defined in appendix A.

This theorem provides existence of the perturbed solution, which directly proves item (i) of theorem 2.1. The norm mentioned there is the weighted Sobolev norm $H'^2_{-1/2}$. By construction, the solution obtained is axially symmetric. It is also maximal, since the tensor (22) is trace free. That proves item (iii). To prove item (ii) we note that by hypothesis the perturbation ω vanishes at the axis, and hence the angular momentum of the family of initial data is the same as in the unperturbed extreme Kerr's data (see the discussion in [22]). The perturbation u lies in the Sobolev space $H'^2_{-1/2}$ and hence (see lemma A.1) it decays at infinity and at the origin as $o(r^{-1/2})$. The decay of u as $r \to \infty$ ensures that the perturbation is asymptotically flat at infinity. Note that the perturbation will change the mass of the original extreme Kerr data since this decay condition allows a non-zero $O(r^{-1})$ term for u. On the other hand, the behavior of u at the origin ensures that it does not modify the cylindrical geometry of the extreme Kerr initial data, since it has a stronger decay rate there. Recall that for the unperturbed conformal factor we have $\lim_{r\to 0} \sqrt{r}\Phi_0 = g(\theta) > 0$ (see equation (B.10)). In particular, the area of the cylindrical end (which is determined by the integral of the function $g(\theta)$) is preserved by the perturbations. That is, the area does not depend on λ.

Proof. The proof uses the implicit function theorem (see theorem C.1 in appendix C; in the rest of the proof we will follow the notation introduced in that theorem) for the map G defined in equation (32). The proof is divided into two steps.

In the first step, we find the appropriate Banach spaces X, Y and Z required by theorem C.1, together with the neighborhoods $U \subset X$ and $V \subset Y$, such that $G : V \times U \to Z$ defines a C^1 map. The delicate part of this step is to take into account in the definition of the Banach spaces the fall-off behavior at infinity and the singular behavior at the origin of the background functions Φ_0, q_0 and ω_0. In particular, it is clear from the equation that we cannot expect the solution u to be regular at the origin, and hence standard Sobolev spaces are not appropriate. Also the presence of the singular background functions Φ_0, q_0 and ω_0 in the map G prevents one from using standard theorems (for example the chain rule in Sobolev spaces) to prove that G is C^1. We need to explicitly compute the functional partial derivatives from their very definition as a limit. This makes this part of the proof laborious. The asymptotic behavior of the background Kerr's functions is typical of any data with one asymptotically flat end and one cylindrical end and that is the main ingredient needed in this step.

In the second step, we prove that the derivative $D_2G(0, 0)$ is an isomorphism between Y and Z. In this part we use very specific properties of extreme Kerr initial data (namely, lemma B.1) which are not valid for generic cylindrical data. See the comment after the proof of lemma B.1. This step represents the key part of the proof.

Step 1. To handle both the fall-off behavior at infinity and the singular behavior at the origin of the functions Φ_0, q_0 and ω_0 we will make use of weighted Sobolev spaces defined in appendix A. We choose $X = \mathbb{R}$, $Y = H'^2_{-1/2}$ and $Z = L'^2_{-5/2}$. We also choose $U = \mathbb{R}$. It is clear that the map G is only defined when $\Phi_0 + u > 0$. Hence, we need to find an appropriate neighborhood

V of 0 in the Banach space Y such that this condition is satisfied. Let us consider V given by the open ball

$$||u||_{H'^2_{-1/2}} < \xi, \tag{33}$$

where the constant ξ is computed as follows. From lemma A.1 we have that for $u \in V$,

$$\sqrt{r}|u| \leqslant C_0\xi, \tag{34}$$

where the constant C_0 is a Sobolev constant independent of u. By lemma B.2 we have

$$\sqrt{r}\Phi_0 \geqslant \sqrt{m}. \tag{35}$$

Then, if we choose ξ such that

$$\frac{\sqrt{m}}{C_0} > \xi > 0, \tag{36}$$

we have that for all $u \in V$,

$$\sqrt{r}(\Phi_0 + u) \geqslant \sqrt{m} - C_0\xi > 0. \tag{37}$$

The constant ξ will remain fixed for the rest of the proof.

We first prove that $G : \mathbb{R} \times V \to L'^2_{-5/2}$ is well defined as a map. That is, we need to check that for $\lambda \in \mathbb{R}$ and $u \in V$ we obtain $G(\lambda, u) \in L'^2_{-5/2}$. Let us compute the norm $L'^2_{-5/2}$ of $G(\lambda, u)$. Using the definition (32) and the triangle inequality, we get

$$\begin{aligned}\|G(\lambda,u)\|_{L'^2_{-5/2}} \leqslant \|\Delta u\|_{L'^2_{-5/2}} &+ \left\| \frac{\lambda\partial\omega\,(2\partial\omega_0 + \lambda\partial\omega)}{16\rho^4(\Phi_0+u)^7} \right\|_{L'^2_{-5/2}} \\ &+ \frac{\lambda}{4}\,\|(\Phi_0+u)\Delta_2 q\|_{L'^2_{-5/2}} \\ &+ \left\| \frac{(\partial\omega_0)^2}{16\rho^4}\left[\frac{1}{(\Phi_0+u)^7} - \frac{1}{\Phi_0^7}\right]\right\|_{L'^2_{-5/2}} + \frac{1}{4}\,\|u\Delta_2 q_0\|_{L'^2_{-5/2}}\,.\end{aligned} \tag{38}$$

From the definition of the $H'^2_{-1/2}$-norm it is clear that the first term on the right-hand side of (38) is bounded. For the second and third terms we use the hypothesis that ω has compact support outside the axis and q compact support outside the origin together with the lower bound (37) to conclude that these terms are also bounded. The delicate terms are the last two.

For the fourth term we proceed as follows. Using the following elementary identity for real numbers a and b:

$$\frac{1}{a^p} - \frac{1}{b^p} = (b-a)\sum_{i=0}^{p-1} a^{i-p}b^{-1-i}, \tag{39}$$

we find that

$$r^{-4}\left(\frac{1}{\Phi_0^7} - \frac{1}{(\Phi_0+u)^7}\right) = uH, \tag{40}$$

where H is given by

$$H = \sum_{i=0}^{6}(\sqrt{r}(\Phi_0+u))^{i-7}(\sqrt{r}\Phi_0)^{-1-i}. \tag{41}$$

Using inequalities (35) and (37) we obtain

$$H \leqslant C, \tag{42}$$

where the constant C depends only on the mass parameter m of the background extreme Kerr solution. In the following we will generically denote by C constants depending at most on m. Then, we have

$$\left\| \frac{(\partial\omega_0)^2}{\rho^4}\left[\frac{1}{(\Phi_0+u)^7}-\frac{1}{\Phi_0^7}\right]\right\|_{L'^2_{-5/2}} \leqslant \left\| \frac{C}{r^6}(r^4 u H)\right\|_{L'^2_{-5/2}} \tag{43}$$

$$= C\,\|u\|_{L'^2_{-1/2}} \leqslant C\,\|u\|_{H'^2_{-1/2}}\,. \tag{44}$$

Where we have used the bound (B.20) in lemma B.2 to bound the factor with ω_0 in the first inequality in (43). The last inequality in (43) comes from the definition of the weighted Sobolev space $H'^2_{-1/2}$.

For the fifth term, which involves q_0, we use the bound (B.21) in lemma B.2, to find

$$\|u\Delta_2 q_0\|_{L'^2_{-5/2}} \leqslant C\left\|\frac{u}{r^2}\right\|_{L'^2_{-5/2}} = C\,\|u\|_{L'^2_{-1/2}} \leqslant C\,\|u\|_{H'^2_{-1/2}}\,. \tag{45}$$

These computations show that all norms involved in $\|G(\lambda,u)\|_{L'^2_{-5/2}}$ are finite; hence, $G:\mathbb{R}\times V\to L'^2_{-5/2}$ is a well-defined map.

We will now prove that G is C^1 between the mentioned Sobolev spaces. Let us denote by $D_1G(\lambda,u)$ the partial Fréchet derivative of G with respect to the first argument evaluated at (λ,u) and by $D_2G(\lambda,u)$ the partial derivative with respect to the second argument. By definition, the partial derivatives are linear operators between the following spaces:

$$D_1G(\lambda,u):\mathbb{R}\to L'^2_{-5/2}, \tag{46}$$

$$D_2G(\lambda,u):H'^2_{-1/2}\to L'^2_{-5/2}. \tag{47}$$

We use the notation $D_1G(\lambda,u)[\gamma]$ to denote the operator $D_1G(\lambda,u)$ acting on $\gamma\in\mathbb{R}$. That is, $D_1G(\lambda,u)[\gamma]$ defines a function on $L'^2_{-5/2}$. In the same way we denote by $D_2G(\lambda,u)[v]$ the operator acting on a function $v\in H'^2_{-1/2}$.

We propose as candidates for these partial derivatives the following linear operators:

$$D_1G(\lambda,u)[\gamma]=\left(\frac{2(\partial w_0+\lambda\partial w)\cdot\partial w}{16\rho^4(\Phi_0+u)^7}+\frac{\Delta_2 q}{4}(\Phi_0+u)\right)\gamma, \tag{48}$$

$$D_2G(\lambda,u)[v]=\Delta v+\left(-\frac{7(\partial w_0+\lambda\partial w)^2}{16\rho^4(\Phi_0+u)^8}+\lambda\frac{\Delta_2 q}{4}+\frac{\Delta_2 q_0}{4}\right)v. \tag{49}$$

These operators arise by taking formally the following directional derivatives to the map G:

$$\frac{\mathrm{d}}{\mathrm{d}t}G(\lambda+t\gamma,u)|_{t=0}=D_1G(\lambda,u)[\gamma], \tag{50}$$

$$\frac{\mathrm{d}}{\mathrm{d}t}G(\lambda,u+tv)|_{t=0}=D_2G(\lambda,u)[v]. \tag{51}$$

To prove that the map $G:\mathbb{R}\times V\to Z$ is C^1 we need to prove the following items.

(i) The linear operators (48) and (49) are bounded, namely

$$\|D_1G(\lambda,u)[\gamma]\|_{L'^2_{-5/2}}\leqslant C_1|\gamma|, \tag{52}$$

$$\|D_2G(\lambda,u)[v]\|_{L'^2_{-5/2}}\leqslant C_2\,\|v\|_{H'^2_{-1/2}}\,, \tag{53}$$

where the constants C_1 and C_2 do not depend on γ and v, respectively.

(ii) The operators (48) and (49) are continuous in (λ, u) with respect to the operator norms. That is, for every $\delta > 0$ there exists $\epsilon > 0$ such that

$$|\lambda_1 - \lambda_2| < \epsilon \Rightarrow \|D_1 G(\lambda_1, u) - D_1 G(\lambda_2, u)\|_{\mathcal{L}(X,Z)} < \delta \tag{54}$$

and

$$\|u_1 - u_2\|_{H^2_{-1/2}} < \epsilon \Rightarrow \|D_1 G(\lambda, u_1) - D_1 G(\lambda_2, u_2)\|_{\mathcal{L}(Y,Z)} < \delta, \tag{55}$$

where the operator norms used on the right-hand side of these inequalities are defined in appendix C.

(iii) The operators (48) and (49) are the partial Fréchet derivatives of G (see the definition in appendix C). That is,

$$\lim_{\gamma \to 0} \frac{\|G(\lambda + \gamma, u) - G(\lambda, u) - D_1 G(\lambda, u)[\gamma]\|_{L^2_{-5/2}}}{|\gamma|} = 0 \tag{56}$$

and

$$\lim_{v \to 0} \frac{\|G(\lambda, u + v) - G(\lambda, u) - D_2 G(\lambda, u)[v]\|_{L^2_{-5/2}}}{\|v\|_{H^2_{-1/2}}} = 0. \tag{57}$$

By performing similar computations as above it is straightforward to prove (i) and also the following estimate:

$$\|D_1 G(\lambda_1, u) - D_1 G(\lambda_2, u)\|_{L^2_{-5/2}} \leqslant C|\lambda_1 - \lambda_2|, \tag{58}$$

where C does not depend on λ_1 and λ_2. From inequality (58) the continuity with respect to λ follows equation (54) of item (ii). In fact, estimate (58) is a bit stronger since it gives uniform continuity.

Continuity in the u direction is more delicate. Using again the identity (39) we have

$$r^{-9/2}\left(\frac{1}{(\Phi_0 + u_1)} - \frac{1}{(\Phi_0 + u_2)}\right) = (u_2 - u_1)H, \tag{59}$$

where

$$H = \sum_{i=0}^{7} (\sqrt{r}(\Phi_0 + u_1))^{i-8} (\sqrt{r}(\Phi_0 + u_2))^{-1-i}. \tag{60}$$

Using that $u_1, u_2 \in V$ and the lower bound (37) we obtain

$$H \leqslant C. \tag{61}$$

We use the upper bound (B.20), together with (61) to find

$$\|D_1 G(\lambda, u_1) - D_1 G(\lambda_2, u_2)\|_{L^2_{-5/2}} \leqslant C \left\| \frac{v(u_1 - u_2)}{r^{3/2}} \right\|_{L^2_{-5/2}}. \tag{62}$$

We bound the right-hand side of (62) as follows

$$\left\| \frac{v(u_1 - u_2)}{r^{3/2}} \right\|_{L^2_{-5/2}} = \left(\int_{\mathbb{R}^3} \frac{v^2 (u_1 - u_2)^2}{r} \, \mathrm{d}x \right)^{1/2}, \tag{63}$$

$$= \left(\int_{\mathbb{R}^3} \frac{(\sqrt{r}v)^2 (u_1 - u_2)^2}{r^2} \, \mathrm{d}x \right)^{1/2} \tag{64}$$

$$\leqslant C \, \|v\|_{H^2_{-1/2}} \left(\int_{\mathbb{R}^3} \frac{(u_1 - u_2)^2}{r^2} \, \mathrm{d}x \right)^{1/2} \tag{65}$$

$$\leqslant C \|v\|_{H'^2_{-1/2}} \|u_1 - u_2\|_{H'^2_{-1/2}}. \tag{66}$$

Equation (63) is just the definition of the $L'^2_{-5/2}$-norm and equation (64) is a trivial rearrangement of factors. The crucial inequality is (65) where we have used lemma A.1. Finally, line (66) trivially follows from the definition of $H'^2_{-1/2}$-norms. Hence, we obtain our final inequality

$$\|D_1 G(\lambda, u_1) - D_1 G(\lambda_2, u_2)\|_{L'^2_{-5/2}} \leqslant C \|v\|_{H'^2_{-1/2}} \|u_1 - u_2\|_{H'^2_{-1/2}}. \tag{67}$$

From this inequality, the continuity (55) follows.

We now prove (iii). The first limit (56) is straightforward. The delicate part is the second limit (57). We will follow a similar argument as in the previous calculation. We first compute

$$G(\lambda, u+v) - G(\lambda, u) - D_2 G(\lambda, u)[v] = \frac{(\partial\omega_0 + \lambda\partial\omega)^2}{16\rho^4} \left(\frac{1}{(\Phi_0 + u + v)^7} - \frac{1}{(\Phi_0 + u)^7} + \frac{7v}{(\Phi_0 + u)^8} \right). \tag{68}$$

We have

$$r^{-9/2} \left(\frac{1}{(\Phi_0 + u + v)^7} - \frac{1}{(\Phi_0 + u)^7} + \frac{7v}{(\Phi_0 + u)^8} \right) = v^2 H, \tag{69}$$

with

$$H = \frac{1}{(\sqrt{r}(\Phi_0 + u + v))^7 (\sqrt{r}(\Phi_0 + u))^8} \sum_{\substack{i+j+k=6 \\ i,j,k \geqslant 0}} C_{ijk} (\sqrt{r}\Phi_0)^i (\sqrt{r}u)^j (\sqrt{r}v)^k, \tag{70}$$

where C_{ijk} are numerical constants. To bound H we use the upper and lower bounds for Φ_0 given by (B.19) and the fact that $u, v \in V$ (and hence they satisfy the bound (34)). We obtain

$$|H| \leqslant C \frac{(r+m)^{6/2}}{(\sqrt{(r+m)} - C_0\xi)^{15}} \leqslant C. \tag{71}$$

Then, we have

$$\|G(\lambda, u+v) - G(\lambda, u) - D_2 G(\lambda, u)[v]\|_{L'^2_{-5/2}} \leqslant C \left\| \frac{r^{9/2} v^2 H}{r^6} \right\|_{L'^2_{-5/2}}, \tag{72}$$

$$= \left\| \frac{v^2}{r^{3/2}} \right\|_{L'^2_{-5/2}}. \tag{73}$$

Using the same argument as we used in equations (63)–(66) we finally get the desired estimate

$$\|G(\lambda, u+v) - G(\lambda, u) - D_2 G(\lambda, u)[v]\|_{L'^2_{-5/2}} \leqslant C \left(\|v\|_{H'^2_{-1/2}} \right)^2. \tag{74}$$

From (74) it follows (57).

Step 2. We will prove that $D_2 G(0,0) : H'^2_{-1/2} \to L'^2_{-5/2}$ is an isomorphism. We write this linear operator in the following form:

$$D_2 G(0,0)[v] = \Delta v - \alpha v, \tag{75}$$

where

$$\alpha = 7 \frac{(\partial\omega_0)^2}{16\rho^4 \Phi_0^8} - \frac{\Delta_2 q_0}{4}. \tag{76}$$

By lemma B.1 we have that $\alpha = hr^{-2}$ where h is a positive and bounded function in $\mathbb{R}^3$. In [26] it has been proved that under such conditions for α the map (75) is an isomorphism between $H'^2_{-1/2}$ and $L'^2_{-5/2}$.

We have satisfied all the hypothesis of the implicit function theorem. Hence, there exists a neighborhood $W = (-\lambda_0, \lambda_0)$ of the origin in $\mathbb{R}$ such that the conclusion of theorem 3.1 holds.

Remarks. We have imposed the perturbation functions ω and q to have compact support. This can be relaxed by requiring appropriate fall off conditions at the axis and at the origin.

The axially symmetric data considered here are not the most general ones, since we are assuming in the form of the metric (21) that the axial Killing vector is hypersurface orthogonal on the surface S (but, of course, has a non-zero twist in the spacetime). This simplification allows one to use the explicit expressions (22) for the second fundamental form. We expect that this result can be generalized without this assumption. However, it is important to emphasize that given data such as that constructed in this theorem, the time evolution described in section 2, under the condition for lapse and shift (19)–(20), will develop initial data with the same asymptotic geometry for which the Killing vector is not surface orthogonal. And hence we get from our family also non-trivial initial data for which the Killing vector is not hypersurface orthogonal.

4. Final comments

We have proven the existence of an initial data family close to extreme Kerr black hole initial data. This family represents the natural initial data to study the evolution near an extreme black hole in axial symmetry, in the spirit of [20, 25].

There also exist relevant open problems that can be addressed at the level of the initial data. As we have seen in section 2, the extreme Kerr black hole data lie outside the black hole region and hence they contain no trapped surfaces. Does the family $(S, h_{ij}(\lambda), K_{ij}(\lambda))$ contains trapped surfaces for $\lambda > 0$? If these data have no trapped surfaces, then there is a chance that they also lie outside the black hole region. This can, of course, only be answered after the whole evolution has been analyzed. On the other hand, if there are trapped surfaces, then the data necessarily penetrate the black hole. The formation of trapped surfaces for arbitrary small $\lambda > 0$ will indicate that extreme Kerr data are a very special element in the family $(S, h_{ij}(\lambda), K_{ij}(\lambda))$. In that case, this kind of data could be very useful in the study of geometric inequalities which relate angular momentum and area of trapped surfaces (see section 8 in the review article [33]).

Acknowledgments

SD thanks Piotr Chruściel and Raffe Mazzeo for useful discussions. The discussions with P Chruściel took place at the Institut Mittag-Leffler, during the program 'Geometry, Analysis, and General Relativity', 2008 fall. The discussions with R Mazzeo took place at the Mathematisches Forschungsinstitut Oberwolfach during the workshop 'Mathematical Aspects of General Relativity', 11–17 October 2009. SD thanks the organizers of these events for the invitation and the hospitality and support of the Institut Mittag-Leffler and Mathematisches Forschungsinstitut Oberwolfach. The authors want to thank Robert Beig for useful discussions that took place at FaMAF during his visit in 2009. SD is supported by CONICET (Argentina). MEGC is supported by a fellowship of CONICET (Argentina). This work was supported in part by grant PIP 6354/05 of CONICET (Argentina), grant 05/B415 Secyt-UNC (Argentina)

and the Partner Group grant of the Max Planck Institute for Gravitational Physics, Albert-Einstein-Institute (Germany).

Appendix A. Weighted Sobolev spaces

The Bartnik's weighted Sobolev spaces $W'^{k,p}_{\delta}$ [5] are appropriate for studying geometries with one cylindrical and one asymptotically flat end. These functional spaces have weights both at infinity and at the origin.

The weighted Lebesgue spaces L'^{p}_{δ} are defined as the completion of $C^{\infty}_{0}(\mathbb{R}^n\setminus\{0\})$ functions under the norms

$$\|f\|'_{p,\delta} = \left(\int_{\mathbb{R}^3\setminus\{0\}} |f|^p r^{-\delta p-n}\,\mathrm{d}x\right)^{1/2}. \tag{A.1}$$

The weighted Sobolev spaces $W'^{k,p}_{\delta}$ are defined in the usual way

$$\|f\|'_{k,p,\delta} = \sum_{0}^{m} \|D^j f\|_{p,\delta-j}. \tag{A.2}$$

In this paper we only use the cases $n = 3$ and $p = 2$; we have denoted these spaces by $H'^{k}_{\delta} = W'^{k,2}_{\delta}$ and the norms by $\|f\|_{L^2_\delta} = \|f\|'_{2,\delta}$ and $\|f\|_{H'^{k}_{\delta}} = \|f\|'_{k,2,\delta}$.

The next lemma plays a crucial role in the proof of theorem 3.1.

Lemma A.1. *Assume $u \in W'^{k,p}_{\delta}$ with $n - kp < 0$; then we have the following estimate:*

$$r^{-\delta}|u| \leqslant C\,\|u\|'_{k,p,\delta}\,. \tag{A.3}$$

Moreover, we have

$$\lim_{r\to 0} r^{-\delta}|u| = \lim_{r\to\infty} r^{-\delta}|u| = 0. \tag{A.4}$$

We will use this lemma only for the particular cases $p = 2$, $n = 3$, $k = 2$ and $\delta = -1/2$; we state however the proof for the general case since it can have other applications.

Proof. This proof is adapted from [5], theorem 1.2, where the statement is proved for weighted spaces at infinity (namely, $W^{k,p}_{\delta}$ spaces in the notation of [5]).

Let B_R be the ball of radius R centered at the origin, and let A_R be the annulus $A_R = B_{2R}\setminus B_R$. We define the rescaled function

$$u_R(x) := u(Rx). \tag{A.5}$$

Then, the fundamental scaling property of the spaces $W'^{k,p}_{\delta}$ (cf the equation after equation (1.3) in [5]) is given by

$$\|u_R\|_{k,p,\delta;A_1} = R^{\delta}\|u\|_{k,p,\delta;A_R}, \tag{A.6}$$

where we have used the same notation as in [5] for norms over subsets of $\mathbb{R}^n$.

We have

$$\sup_{A_R} r^{-\delta}|u| = \sup_{A_1} R^{-\delta} r^{-\delta}|u_R|, \tag{A.7}$$

$$\leqslant CR^{-\delta}\|r^{-\delta}u_R\|_{k,p;A_1}, \tag{A.8}$$

$$\leqslant CR^{-\delta}\|u_R\|'_{k,p,\delta;A_1}, \tag{A.9}$$

$$= C\|u\|'_{k,p,\delta;A_R}. \tag{A.10}$$

The line (A.7) is a trivial change of coordinates. For inequality (A.8) we have used the standard Sobolev estimate on the bounded domain A_1, which is valid for $n - kp < 0$. We have denoted the standard Sobolev norm on a domain Ω by $\|\cdot\|_{k,p;\Omega}$. It is important to note that the constant C does not depend on R, since the domain A_1 does not either. The inequality in (A.9) is trivial because on the domain A_1 the two norms (standard and weighted) are equivalent. Finally, in (A.10) we applied the scaling property (A.6).

Consider the set of annulus A_{2^j} and define $u_j = u|_{A_{2^j}}$. It is clear that

$$u = \sum_{j=-\infty}^{\infty} u_j. \tag{A.11}$$

Then, we use the estimate (A.7) on A_{2^j} and sum over all j:

$$(\sup r^{-\delta}|u|)^p \leqslant \sum_{j=-\infty}^{\infty} (\sup r^{-\delta}|u_j|)^p \leqslant C \sum_{j=-\infty}^{\infty} \|u_j\|'^p_{k,p,\delta}, \tag{A.12}$$

$$= C\|u\|'^p_{k,p,\delta} \tag{A.13}$$

which proves (A.3).

To prove (A.4) we observe that the sum $\sum_{j=-\infty}^{\infty}(\sup r^{-\delta}|u_j|)^p$ is an infinite sum of positive real numbers which is bounded; hence, in the limit we must have

$$\lim_{j\to\pm\infty} (\sup r^{-\delta}|u_j|) = 0, \tag{A.14}$$

which is equivalent to (A.4). □

Appendix B. Properties of extreme Kerr initial data

The spacetime metric for extreme Kerr black hole in Boyer–Lindquist coordinates $(t, \tilde{r}, \theta, \phi)$ is given by

$$g = -\frac{\Delta \sin^2\theta}{\eta}\,\mathrm{d}t^2 + \eta(\mathrm{d}\phi - \Omega\,\mathrm{d}t)^2 + \frac{\Sigma}{\Delta}\,\mathrm{d}\tilde{r}^2 + \Sigma\,\mathrm{d}\theta^2 \tag{B.1}$$

where η is the square norm of the axial Killing vector

$$\eta^\mu = \left(\frac{\partial}{\partial\phi}\right)^\mu, \qquad \eta = g_{\nu\mu}\eta^\mu\eta^\mu, \tag{B.2}$$

given by

$$\eta = \frac{(\tilde{r}^2 + a^2)^2 - a^2\Delta\sin^2\theta}{\Sigma}\sin^2\theta. \tag{B.3}$$

The functions Δ and Σ are given by

$$\Delta = (\tilde{r} - m)^2, \qquad \Sigma = \tilde{r}^2 + a^2\cos^2\theta, \tag{B.4}$$

and Ω is the angular velocity

$$\Omega = \frac{2a^2\tilde{r}\sin^2\theta}{\eta\Sigma}. \tag{B.5}$$

Here $a = J/m$ is the angular momentum per unit mass, and we consider the extreme case $\sqrt{|J|} = m$. Note that for extreme Kerr we have two possible values for the angular momentum $J = \pm m^2$ (and hence $a = \pm m$).

Take a surface $t =$ constant, define the radius r as $r = \tilde{r} - m$. From (B.1) we deduce that the intrinsic metric on this surface has the form (5) with

$$e^{2q_0} = \frac{\Sigma \sin^2\theta}{\eta}, \qquad \Phi_0^4 = \frac{\eta}{\rho^2}. \tag{B.6}$$

The twist potential of the Killing vector η^μ is given by

$$\omega_0 = 2J(\cos^3\theta - 3\cos\theta) - \frac{2Jm^2\cos\theta\sin^4\theta}{\Sigma}. \tag{B.7}$$

The lapse function and shift vector for this foliation are given by

$$\alpha = \frac{r}{\sqrt{\Sigma + a^2(1 + 2a(r+a)/\Sigma)\sin^2\theta}}, \tag{B.8}$$

$$\beta^\phi = -\frac{2a^2\sin^2\theta(r+a)}{\Sigma^3}r^2. \tag{B.9}$$

The following asymptotic limits are interesting:

$$\lim_{r\to 0}\sqrt{r}\Phi_0 = \left(\frac{4m^2}{1+\cos^2\theta}\right)^{1/4}, \tag{B.10}$$

$$\lim_{r\to 0} e^{2q_0} = \left(\frac{1+\cos^2\theta}{2}\right)^2, \tag{B.11}$$

$$\lim_{r\to 0}\omega_0 = -\frac{8J\cos\theta}{1+\cos^2\theta}, \tag{B.12}$$

$$\lim_{r\to 0} R = \frac{2\sin^2\theta}{m^2(1+\cos^2\theta)^3}. \tag{B.13}$$

We take the opportunity to correct a misprint in equation (A.15) of [2]. There is a missing exponent 3 in the denominator of this formula; it should be the same as equation (B.13).

In the following, we use Δ to denote the flat Laplace operator in three dimensions; the two-dimensional Laplacian Δ_2 is given by

$$\Delta_2 = \frac{1}{r}\partial_r(r\partial_r) + \frac{1}{r^2}\partial_\theta^2. \tag{B.14}$$

The next lemma plays a crucial role in the proof of theorem 3.1.

Lemma B.1. *Let q_0 and Φ_0 be given by (B.6) and ω_0 by (B.7). Then the function α defined in (76) has the form $\alpha = hr^{-2}$ where $h \geqslant 0$ and h is bounded in $\mathbb{R}^3$.*

Proof. From the Hamiltonian constraint

$$-\frac{\Delta_2 q_0}{4} = \frac{\Delta\Phi_0}{\Phi_0} + \frac{(\partial w_0)^2}{16\eta^2} \tag{B.15}$$

and the stationary equation satisfied by extreme Kerr's initial data (see [2])

$$\frac{\Delta\Phi_0}{\Phi_0} = -\frac{(\partial\omega_0)^2}{4\eta^2} + \frac{(\partial\Phi_0)^2}{\Phi_0^2} \tag{B.16}$$

we obtain

$$-\frac{\Delta_2 q_0}{4} = -\frac{3}{16}\frac{(\partial w_0)^2}{\eta^2} + \frac{(\partial\Phi_0)^2}{\Phi_0^2}. \tag{B.17}$$

Therefore,

$$\alpha = \frac{(\partial\omega_0)^2}{4\eta^2} + \frac{(\partial\Phi_0)^2}{\Phi_0^2}, \tag{B.18}$$

which is clearly a non-negative quantity. By an explicit calculation it can be seen that α is in fact a strictly positive function. Since we do not need this property for our purposes, we omit the details. Also by explicit means, we note that α is $O(r^{-2})$ at the origin, and $O(r^{-4})$ at infinity, being otherwise bounded. Thereby, there must exist a positive function h such that $\alpha = hr^{-2}$. □

It is important to note that in the proof of lemma B.1 we have used the fact that extreme Kerr satisfies the stationary Einstein equations and also that the topology of extreme Kerr allows us to choose these coordinates. In particular, the proof fails for non-extreme Kerr. See a similar discussion in [19] at the end of p 6868.

Lemma B.2. *Let Φ_0, q_0 and ω_0 be defined by (B.6) and (B.7), and assume that $m > 0$. Then we have the following bounds:*

$$\sqrt{m} \leqslant \sqrt{r+m} \leqslant \sqrt{r}\Phi_0 \leqslant \sqrt{2}\sqrt{r+m}, \tag{B.19}$$

$$\frac{(\partial\omega_0)^2}{\rho^4} \leqslant 116\frac{m^4}{r^6}, \tag{B.20}$$

$$|\Delta_2 q_0| \leqslant \frac{90}{r^2}. \tag{B.21}$$

Proof. Inequality (B.19) has been proved in [2] (see equations (10) and (12) in this reference).

We have

$$(\partial\omega_0)^2 = \frac{4m^4\rho^6 F}{r^8\Sigma^4} \tag{B.22}$$

where

$$F = 4r^2a^4\tilde{r}^2\sin^2(2\theta) + (3\tilde{r}^4 + a^2\tilde{r}^2 + a^2(\tilde{r}^2 - a^2)\cos^2\theta)^2 \tag{B.23}$$

and $\tilde{r} = r + m$. Then,

$$F \leqslant 4r^2a^4\tilde{r}^2 + (3\tilde{r}^4 + a^2\tilde{r}^2 + a^2\tilde{r}^2)^2 \leqslant 29(r+a)^8. \tag{B.24}$$

We also find, bounding $\Sigma \geqslant (r+a)^2$ and $\rho \leqslant r$, that

$$(\partial\omega_0)^2 \leqslant \frac{4a^4\rho^4 29(r+a)^8}{r^6(r+a)^8} = 116\frac{m^4}{r^2}. \tag{B.25}$$

Finally, using the explicit expressions for Φ_0 and ω_0 one can check, after a laborious but straightforward calculation, the bound on $|\Delta_2 q_0|$. □

Appendix C. The implicit function theorem

To facilitate the readability of the paper and also to fix the notation, we reproduce in this appendix well-known results on differential calculus in Banach spaces (see, for example, [1, 10], and also the more introductory text books [36, 38]).

Let X and Z be Banach spaces. Let $A : X \to Z$ be a linear bounded operator. We denote by $\mathcal{L}(X, Z)$ the set of all linear and bounded operators from X to Z. The set $\mathcal{L}(X, Z)$ is itself a Banach space with the operator norm defined by

$$\|A\|_{\mathcal{L}(X,Z)} = \sup_{\|x\|\neq 0} \frac{\|A(x)\|_Z}{\|x\|_X}. \tag{C.1}$$

Let x be a point in X and let G be a mapping from a neighborhood of x into Z. Then G is called Fréchet differentiable at the point x if there exists a linear operator $DG(x) \in \mathcal{L}(X, Z)$ such that

$$\lim_{v\to 0} \frac{\|G(x+v) - G(x) - DG(x)[v]\|}{\|x\|_X} = 0. \tag{C.2}$$

The map G is called continuously differentiable (i.e. C^1) if the derivative $DG(x)$ as an element of $\mathcal{L}(X, Z)$ depends continuously on x. Namely, for every $\delta > 0$ there exists $\epsilon > 0$ such that

$$\|x_1 - x_2\|_X < \epsilon \Rightarrow \|DG(x_1) - DG(x_2)\|_{\mathcal{L}(X,Z)} < \delta. \tag{C.3}$$

Let X, Y and Z be Banach spaces and let G be a map $G : X \times Y \to Z$; in a similar way, we define the partial derivatives with respect to the first argument by $D_1G(x, y)$ and with respect to the second argument by $D_2G(x, y)$.

Theorem C.1 (Implicit function theorem)**.** *Suppose U is a neighborhood of 0 in X, V is a neighborhood of 0 in Y and $G : X \times Y \to Z$ is C^1. Suppose $G(0, 0) = 0$ and $D_2G(0, 0) : Y \to Z$ define a bounded operator and it is an isomorphism. Then, there exists a neighborhood W of the origin in X and a continuously differentiable mapping $f : W \to Y$ such that $G(x, f(x)) = 0$. Moreover, for small x and y, $f(x)$ is the only solution y of the equation $G(x, y) = 0$.*

References

[1] Abraham R, Marsden J E and Ratiu T 1988 *Manifolds, Tensor Analysis, and Applications (Applied Mathematical Sciences* vol 75*)* 2nd edn (New York: Springer)

[2] Avila G A and Dain S 2008 The Yamabe invariant for axially symmetric two Kerr black holes initial data *Class. Quantum Grav.* **25** 225002 (arXiv:gr-qc/00805.2754)

[3] Balasubramanian V 2009 Are black holes really two dimensional? *Physics* **2** 102

[4] Bardeen J M and Horowitz G T 1999 The extreme Kerr throat geometry: a vacuum analog of AdS(2) × S(2) *Phys. Rev.* D **60** 104030 (arXiv:hep-th/9905099)

[5] Bartnik R 1986 The mass of an asymptotically flat manifold *Commun. Pure Appl. Math.* **39** 661–93

[6] Bartnik R and Isenberg J 2004 The constraint equations *The Einstein Equations and Large Scale Behavior of Gravitational Fields* ed P T Chruściel and H Friedrich (Basel: Birhäuser) pp 1–38 (arXiv:gr-qc/0405092)

[7] Boyer R H and Lindquist R W 1967 Maximal analytic extension of the Kerr metric *J. Math. Phys.* **8** 265–81

[8] Carter B 1968 Global structure of the Kerr family of gravitational fields *Phys. Rev.* **174** 1559–71

[9] Carter B 1973 Black hole equilibrium states *Black Holes/Les Astres Occlus (École d'Été Physique Théorique, Les Houches, 1972)* (New York: Gordon and Breach) pp 57–214

[10] Choquet-Bruhat Y, de Witt-Mortte C and Dillard-Bleick M 1977 *Analysis, Manifolds and Physics* (Amsterdam: North-Holland)

[11] Choquet-Bruhat Y, Isenberg J and York J W Jr 1999 Einstein constraint on asymptotically euclidean manifolds *Phys. Rev.* D **61** 084034 (arXiv:gr-qc/9906095)

[12] Chruściel P T, Li Y and Weinstein G 2008 Mass and angular-momentum inequalities for axi-symmetric initial data sets: II. Angular-momentum *Ann. Phys.* **323** 2591–613 (arXiv:0712.4064)

[13] Chrusciel P T and Lopes Costa J 2008 On uniqueness of stationary vacuum black holes *Proc. of Géométrie Différentielle, Physique Mathématique, Mathématiques et Société, Astérisque* vol 321 pp 195–265 (arXiv:0806.0016)

[14] Chrusciel P T and Lopes Costa J 2009 Mass, angular-momentum, and charge inequalities for axisymmetric initial data *Class. Quantum Grav.* **26** 235013 (arXiv:0909.5625)

[15] Costa J L 2010 Proof of a Dain inequality with charge *J. Phys. A: Math. Theor.* **43** 285202 (arXiv:0912.0838)

[16] Dain S 2001 Initial data for a head on collision of two Kerr-like black holes with close limit *Phys. Rev.* D **64** 124002 (arXiv:gr-qc/0103030)

[17] Dain S 2004 Trapped surfaces as boundaries for the constraint equations *Class. Quantum Grav.* **21** 555–73 (arXiv:gr-qc/0308009)

[18] Dain S 2006 Proof of the (local) angular momemtum–mass inequality for axisymmetric black holes *Class. Quantum Grav.* **23** 6845–55 (arXiv:gr-qc/0511087)

[19] Dain S 2006 A variational principle for stationary, axisymmetric solutions of Einstein's equations *Class. Quantum Grav.* **23** 6857–71 (arXiv:gr-qc/0508061)
[20] Dain S 2008 Axisymmetric evolution of Einstein equations and mass conservation *Class. Quantum Grav.* **25** 145021 (arXiv:0804.2679)
[21] Dain S 2008 The inequality between mass and angular momentum for axially symmetric black holes *Int. J. Mod. Phys.* D **17** 519–23 (arXiv:0707.3118 [gr-qc])
[22] Dain S 2008 Proof of the angular momentum-mass inequality for axisymmetric black holes *J. Differ. Geom.* **79** 33–67 (arXiv:gr-qc/0606105)
[23] Dain S and Gabach Clément M E 2009 Extreme Bowen–York initial data *Class. Quantum Grav.* **26** 035020 (arXiv:0806.2180)
[24] Dain S, Lousto C O and Zlochower Y 2008 Extra-large remnant recoil velocities and spins from near-extremal Bowen–York-spin black-hole binaries *Phys. Rev.* D **78** 024039 (arXiv:0803.0351)
[25] Dain S and Ortiz O E 2009 On well-posedness, linear perturbations and mass conservation for axisymmetric Einstein equation arXiv:0912.2426
[26] Gabach Clément M E 2010 Conformally flat black hole initial data with one cylindrical end *Class. Quantum Gravity* **27** 125010 (arXiv:0911.0258)
[27] Guica M, Hartman T, Song W and Strominger A 2009 The Kerr/CFT correspondence *Phys. Rev.* D **80** 124008 (arXiv:0809.4266)
[28] Hannam M, Husa S and Murchadha N O 2009 Bowen–York trumpet data and black-hole simulations *Phys. Rev.* D **80** 124007 (arXiv:0908.1063)
[29] Hannam M, Husa S, Ohme F, Bruegmann B and O'Murchadha N 2008 Wormholes and trumpets: the Schwarzschild spacetime for the moving-puncture generation *Phys. Rev.* D **78** 064020 (arXiv:0804.0628)
[30] Immerman J D and Baumgarte T W 2009 Trumpet-puncture initial data for black holes *Phys. Rev.* D **80** 061501 (arXiv:0908.0337)
[31] Isenberg J 1995 Constant mean curvature solution of the Einstein constraint equations on closed manifold *Class. Quantum Grav.* **12** 2249–74
[32] Lovelace G, Owen R, Pfeiffer H P and Chu T 2008 Binary-black-hole initial data with nearly-extremal spins *Phys. Rev.* D **78** 084017 (arXiv:0805.4192)
[33] Mars M 2009 Present status of the Penrose inequality *Class. Quantum Grav.* **26** 193001 (arXiv:0906.5566)
[34] Maxwell D 2005 Solutions of the Einstein constraint equations with apparent horizon boundaries *Commun. Math. Phys.* **253** 561–83 (arXiv:gr-qc/0307117)
[35] McClintock J E, Shafee R, Narayan R, Remillard R A, Davis S W and Li L-X 2006 The spin of the near-extreme Kerr black hole GRS 1915+105 *Astrophys. J.* **652** 518–39
[36] McOwen R C 1996 *Partial Differential Equation* (New Jersey: Prentice-Hall)
[37] Reid M J 2009 Is there a supermassive black hole at the center of the Milky Way? *Int. J. Mod. Phys.* D **18** 889–910 (arXiv:0808.2624)
[38] Renardy M and Rogers R C 2004 *An Introduction to Partial Differential Equations (Texts in Applied Mathematics* vol 13*)* 2nd edn (New York: Springer)